

Understanding the persistence of measles: reconciling theory, simulation and observation

Matt J. Keeling* and Bryan T. Grenfell

Department of Zoology, University of Cambridge, Downing Street, Cambridge CB2 3EJ, UK

Ever since the pattern of localized extinction associated with measles was discovered by Bartlett in 1957, many models have been developed in an attempt to reproduce this phenomenon. Recently, the use of constant infectious and incubation periods, rather than the more convenient exponential forms, has been presented as a simple means of obtaining realistic persistence levels. However, this result appears at odds with rigorous mathematical theory; here we reconcile these differences. Using a deterministic approach, we parameterize a variety of models to fit the observed biennial attractor, thus determining the level of seasonality by the choice of model. We can then compare fairly the persistence of the stochastic versions of these models, using the ‘best-fit’ parameters. Finally, we consider the differences between the observed fade-out pattern and the more theoretically appealing ‘first passage time’.

Keywords: mathematical models; childhood disease; extinctions; stochasticity; seasonality

1. INTRODUCTION

Localized extinctions are a common feature of all small populations and have been observed and modelled for animals (Stacey & Taper 1992; Lande 1993; Hanski *et al.* 1995; Holyoak & Lawler 1996; Ludwig 1996; Sutcliffe *et al.* 1997; Bascompte & Rodriguez-Trelles 1998; Marion *et al.* 2000), plants (Ouborg 1993; Tilman 1994; Swinton & Gilligan 1996) and diseases (Bartlett 1957, 1960; Black 1966; Grenfell 1992; Keeling 1997; van Herwaarden 1997; Caraco *et al.* 1998; Earn *et al.* 1998). In 1957, Bartlett made the seminal observation that the number of localized extinctions, or fade-outs, of measles was related to the population size of the community. Small populations demonstrated many extinctions, whereas large populations showed very few; similar results have also been observed for other diseases and also larger organisms. This led to the notion of the critical community size (CCS), which is defined as the smallest population size that does not exhibit disease extinctions. The CCS has been estimated for a variety of communities, including cities in England and Wales (Bartlett 1957), cities in the United States (Bartlett 1960; Bolker & Grenfell 1996) and isolated islands (Black 1966). Surprisingly, its value is remarkably consistent between datasets, lying between three and five hundred thousand.

Given the robust nature of the CCS and the associated pattern of fade-outs, many researchers have attempted to capture these features using stochastic event-driven models (Bartlett 1956; Grenfell 1992; Grenfell *et al.* 1995; Bolker & Grenfell 1996; Ferguson *et al.* 1997; Keeling 1997; Keeling & Grenfell 1997). However, the persistence of real-world systems is an emergent phenomenon and arises from the interaction between dynamics and stochasticity. Such a phenomenon cannot be built into a model *a priori* and can only be determined by repeated simulation of the stochastic system—although recently some progress

has been made towards more analytical approaches (Andersson & Djehiche 1998; Swinton 1998; Nasell 1999; Andersson & Britton 2000; Keeling 2000). Therefore, each new stochastic model must be simulated and compared with the available fade-out data, which can often be a computationally intensive process.

The earliest models all vastly overestimated the CCS, being unable to demonstrate the levels of persistence observed. More complex stochastic models that included more heterogeneities, such as age-structure or spatial-structure, did far better but still underestimated the amount of persistence (Bolker & Grenfell 1995; Grenfell *et al.* 1995; Ferguson *et al.* 1997; Keeling 1997). In 1997, Keeling and Grenfell proposed a simple modification to the standard models that vastly increased persistence by forcing the incubation and infectious periods to be closer to fixed intervals, rather than the standard exponential distribution that is commonly implemented. These more constant periods agree well with observations of disease transmission within households (Hope-Simpson 1952; Bailey 1956) and demonstrate the high frequency ‘pulsing’ detectable at the start of many epidemics (Keeling & Grenfell 1997).

With such constant periods, however, there appears to be a discrepancy between theory and simulation. Work on SIR-type (susceptible, infectious, recovered) models has shown theoretically that constant periods destabilized disease dynamics (Grossman 1980; Nasse 1999; Andersson & Britton 2000; Lloyd 2001), whereas the numerical simulations of Keeling & Grenfell (1997) showed far greater persistence for these constant periods. This difference between theory and simulation can be resolved by realizing that all models should be able to accurately reproduce the general biennial pattern of measles epidemics observed before vaccination. That is, by forcing a model to be an accurate description of the observed measles dynamics, the parameter values are governed by our choice of model. The previous theoretical work kept the parameters fixed while varying the model and therefore has not necessarily been comparing reliable models of measles.

* Author and address for correspondence: Biological Sciences and/or Mathematics Institute, University of Warwick, Gibbet Hill, Coventry CV4 7AL, UK (matt@zoo.cam.ac.uk).

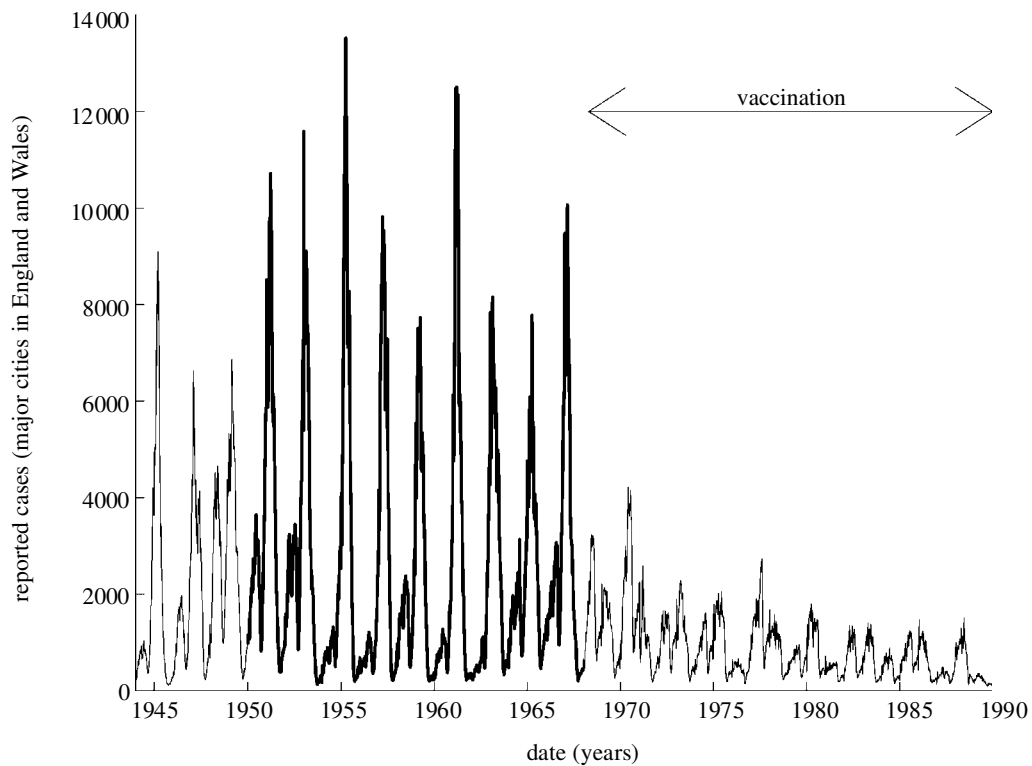


Figure 1. The total number of reported measles cases from the major cities of England and Wales. Biennial cycles are clearly evident from 1950 until vaccination started in the late sixties.

Using deterministic models of various sorts, § 2 explores which parameters provide the best fit to the observed data for each model type. In § 3 we abandon the deterministic framework and use event-driven stochastic models, which is necessary to capture the phenomena of extinction and persistence. With these models we consider two measures of persistence: the average number of extinctions (or fade-outs) per year and the probability of extinction within a given time-frame.

2. FITTING MODELS TO DATA

Between 1950 and 1968, measles in large communities in England and Wales showed a clear biennial signature, with a major epidemic every other year (figure 1). We therefore propose that, before vaccination, measles (as least in England and Wales) had an underlying deterministic 2-year cycle (Schenzle 1984; Anderson & May 1992). In particular, we can find the mean observed biennial pattern X_{obs} and the variance about it, V_{obs} ,

$$X_{\text{obs}}(t) = \frac{1}{9} \sum_{\tau=0}^8 \hat{I}(1950 + 2^* \tau + t) \quad 0 \leq t < 2, \quad (2.1)$$

$$V_{\text{obs}}(t) = \frac{1}{8} \sum_{\tau=0}^8 [\hat{I}(1950 + 2^* \tau + t) - X_{\text{obs}}(t)]^2, \quad (2.2)$$

where $\hat{I}(t)$ is the proportion of the population infectious at that time, as estimated from the number of reported cases. Throughout, we have used data from London (the largest city in the UK) for comparison with our deterministic models.

We now want to compare the results of a deterministic model against the observations and determine a least-

squares fit. If $I^*(t)$ is the proportion of infectious individuals on the deterministic attractor of the model, then we define the error between the model and observations, E_V , to be,

$$E_V = \frac{1}{2} \int_0^2 \frac{(I^*(t) - X_{\text{obs}}(t))^2}{V_{\text{obs}}(t)} dt. \quad (2.3)$$

Note that for mathematical simplicity we have implicitly assumed that the attractor of the deterministic model is biennial. This error, E_V , measures the deviation of the model from the observed attractor relative to the observed variation at that point. As such, minimizing E_V gives a weighted least-squares fit. A second error measure, E_1 , has been used to confirm the generality of the results,

$$E_1 = \frac{1}{2} \int_0^2 (I^*(t) - X_{\text{obs}}(t))^2 dt, \quad (2.4)$$

where, for conformity, we first scale the population size and observed data such that the average number of infectious cases per year is one. This alternative measure of the error is simply the variance about the average observed attractor; hence, minimizing E_1 results in a standard least-squares fit.

Using the two error measures given above, we can now refine the parameters of any given model so as to achieve a good match between the simulated attractor and the observed dynamics. For completeness, we will consider a variety of models, which are composed from three fundamental elements. (Appendix A gives the underlying differential equations that correspond to these deterministic

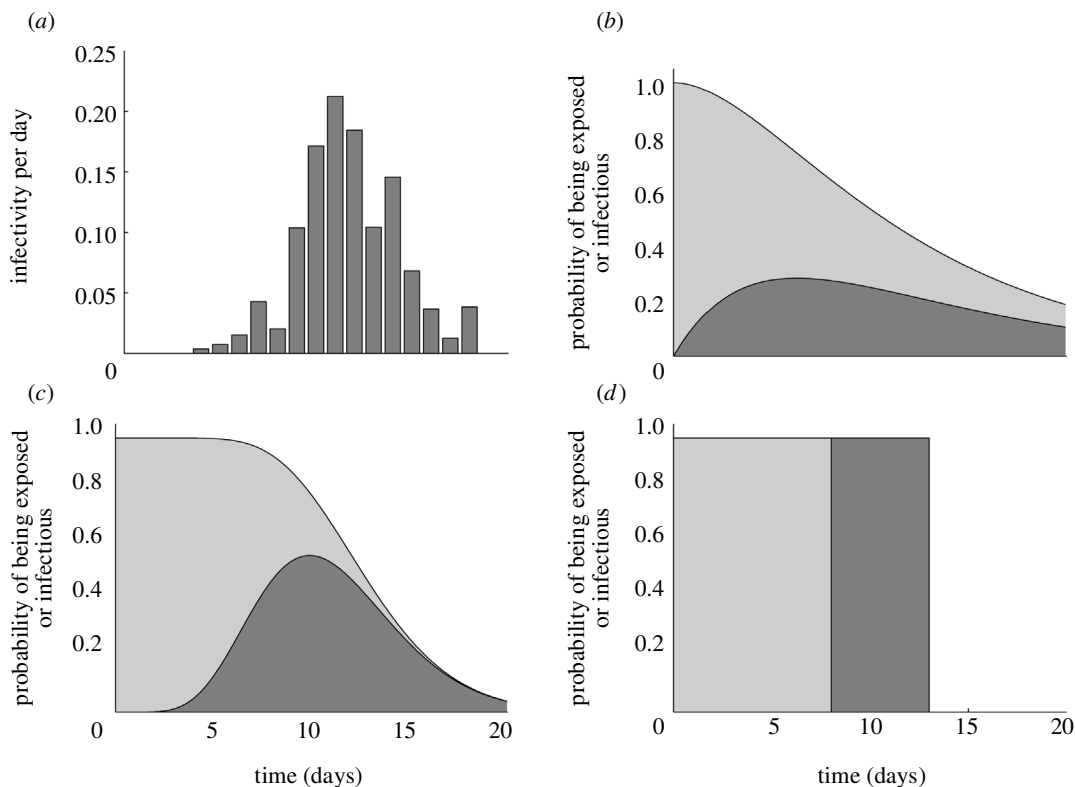


Figure 2. Comparison between household observations and the distribution of infectious period for the three models. (a) The daily probability of infection from households where one individual is infectious and one is susceptible (data from Hope-Simpson 1952; Bailey 1956). (b, c and d) The probability that an individual infected at time zero is exposed (light grey) or infectious (dark grey) at a later time. ((b) exponential SEIR, (c) gamma SEIR and (d) constant SEIR.)

models.) These elements can be assembled in different combinations to generate a multitude of models.

The most basic element is whether measles is modelled as SIR or SEIR (susceptible, exposed, infectious, recovered) (Anderson & May 1992). We insist that the infectious and incubation periods conform to the observed durations (Hope-Simpson 1952; Bailey 1956) so that, for the SIR model, the average infectious period is 13 days, whereas for the SEIR model, the average exposed period is 8 days while the average infectious period is 5 days. Throughout this paper we shall concentrate on the more realistic SEIR-type models, although results are also given for the simpler SIR models. We also stipulate that the value of R_0 , averaged around the attractor, is 17 (see Appendix A), again conforming to observations (Anderson & May 1992).

The second element is the distribution of the infectious (and exposed) periods. Although much of the original theory of epidemics allows a wide range of assumptions about the periods (Kermack & McKendrick 1927), here we concentrate on three distinct forms (figure 2). The periods can either be the standard exponential distributions, derived by individuals moving from the exposed to the infectious class and then into the recovered class at a constant rate (Anderson & May 1979, 1992; May & Anderson 1979); a constant distribution, where all individuals remain exposed or infectious for a fixed amount of time (Keeling & Grenfell 1997); or a gamma distribution, where the exposed and infectious periods are broken down into a series of subclasses through which individuals move at a constant rate (Anderson & Watson 1980; Lloyd

2001). The gamma distribution model allows us to slide continuously from the exponential distribution (where the variance is greatest) to the fixed-period model (where the variance is zero), by increasing the number of subclasses. Here, for convenience, we have chosen the number of subclasses such that an individual spends an average of one day in each subclass.

The final element is the form of the seasonality and again, two approaches are possible. The earliest and mathematically most convenient approach is to use sinusoidal forcing of the contact rate (Aron & Schwartz 1984; Olsen & Schaffer 1990; Rand & Wilson 1991).

$$\beta(t) = b_0(1 + b_1 \sin(2\pi t)). \quad (2.5)$$

Recently, term-time forcing has proved more popular due to its mechanistic derivation and the observation of its signature in the case notification data (Schenzle 1984; Bolker 1993; Earn *et al.* 2000; Finkenstädt & Grenfell 2000),

$$\beta(t) = b_0(1 + b_1 \text{term}(t)), \quad (2.6)$$

where 'term' is -1 during school holidays and $+1$ during term-times. The fact that R_0 is fixed allows us to obtain a value for b_0 ,

$$b_0 = \frac{R_0}{\text{inf. period} \times \langle 1 + b_1 \sin(2\pi t) \rangle} \quad \text{or} \quad (2.7)$$

$$b_0 = \frac{R_0}{\text{inf. period} \times \langle 1 + b_1 \text{term}(t) \rangle},$$

where $\langle \cdot \rangle$ is the geometric average. However, the level of the seasonality, b_1 , is still undetermined.

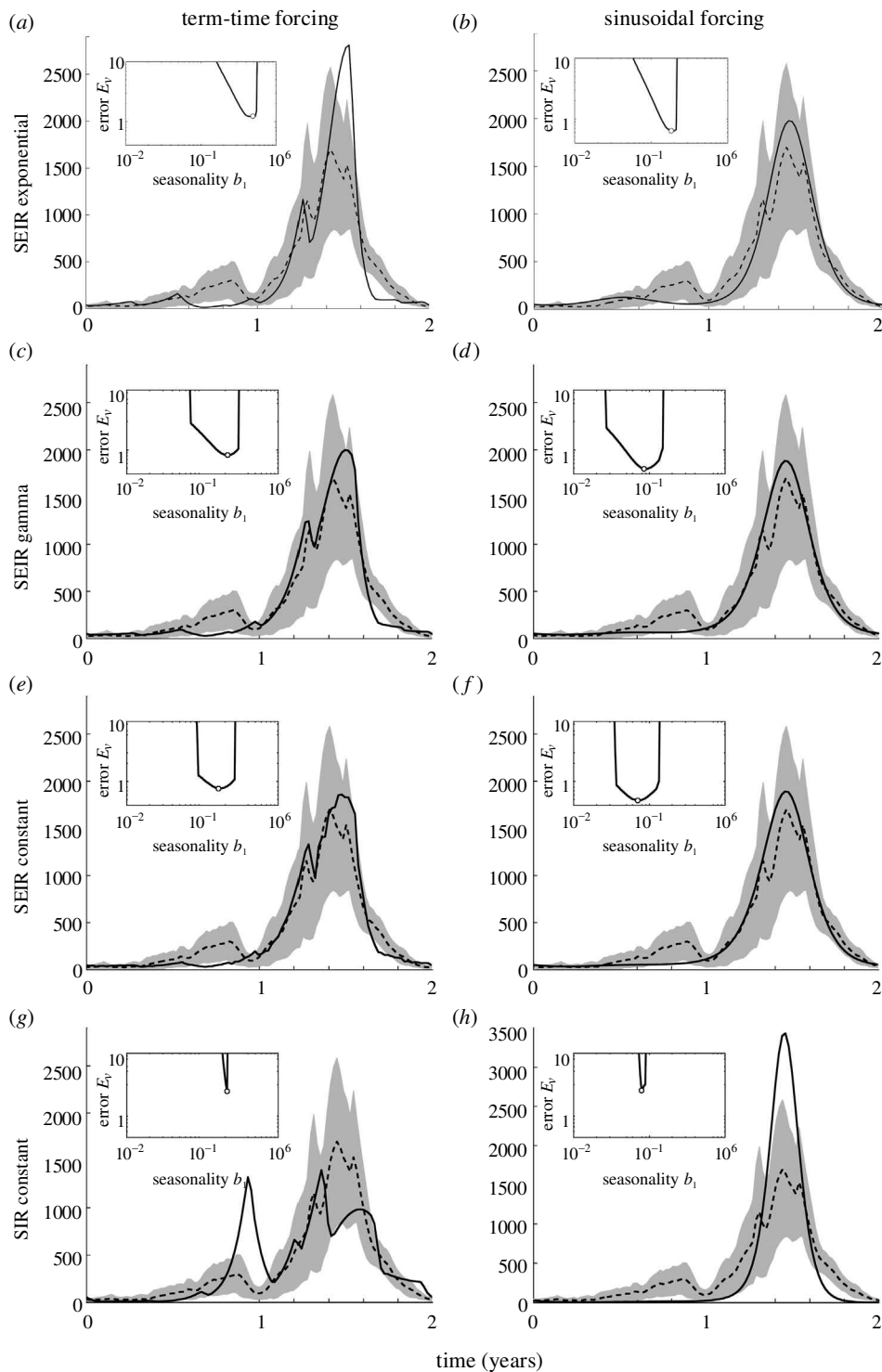


Figure 3. Graphs showing the best fit biennial cycle from four different model types ((a),(b): the standard exponential SEIR; (c),(d): the gamma SEIR; (e),(f): the constant SEIR and (g),(h): the constant SIR) and two types of forcing (the left column is term-time and the right column is a sine wave). The deterministic cycle (solid line) is superimposed on the average biennial cycle from London (dotted line), with the shaded region showing two standard deviations. The inset graphs show the error, E_V , as a function of the seasonal forcing b_1 , the large dot marks the minimum.

We find the appropriate level of seasonality by minimizing the error (obtaining a least squares fit) between the model and the average biennial cycle. Figure 3 compares the average observed epidemic cycle in London, X_{obs} , with the deterministic attractor, I^* , when the error, E_V , is minimized; the inset graphs show this error against the level of seasonality, b_1 . Table 1 gives the numerical values of b_1 that minimize the error for all 12 possible models. Two

key factors emerge. First, the constant period SIR models (figure 3g,h) fail to capture the observed biennial cycle and therefore must be rejected as a model of measles. This failure is interesting because it shows that details can be very important and that the slight delay induced by the exposed period is necessary to capture the dynamics. The second factor is that the standard exponential models require much higher levels of seasonality than the more

Table 1. Optimum level of seasonality, b_1 and the associated error, E , for the six different model types and the two kinds of seasonal forcing.

(Note for comparison that the PRAS model (Keeling & Grenfell 1997) has an error of only $E_V = 0.31$.)

| model | term-time | | | | sinusoidal | | | |
|------------------|-----------|-------|-------|-------|------------|-------|-------|-------|
| | E_V | | E_1 | | E_V | | E_1 | |
| | b_1 | error | b_1 | error | b_1 | error | b_1 | error |
| exponential SIR | 0.55 | 1.02 | 0.32 | 1.56 | 0.20 | 0.64 | 0.12 | 0.84 |
| exponential SEIR | 0.51 | 1.18 | 0.29 | 1.44 | 0.18 | 0.64 | 0.11 | 0.85 |
| gamma SIR | 0.16 | 0.69 | 0.15 | 1.65 | 0.05 | 0.50 | 0.05 | 1.42 |
| gamma SEIR | 0.22 | 0.82 | 0.13 | 1.14 | 0.09 | 0.49 | 0.05 | 0.80 |
| constant SIR | 0.22 | 2.34 | 0.21 | 4.78 | 0.08 | 2.41 | 0.07 | 7.95 |
| constant SEIR | 0.17 | 0.76 | 0.10 | 1.12 | 0.07 | 0.48 | 0.04 | 0.82 |

narrowly distributed periods of the gamma and constant models. This is in agreement with the theory of Grossman (1980) and the results of Lloyd (2001), showing that models with less variability in their infectious and exposed periods are more unstable, and therefore that much lower levels of seasonality are required to excite biennial oscillations. However, we have constrained our model to be a good fit to the observed measles dynamics; hence each model has an associated value of b_1 , and this value must be sufficiently large to produce biennial oscillations but not so large that more complex dynamics arise (Lloyd 2001).

It should be noted that such a method of fitting models to data also has some associated problems. We are fitting the results of a deterministic, homogeneous system of equations to the observations from London, which is inherently stochastic, heterogeneous and may be affected by changes in birth rate, schooling patterns etc. Small variations in the precise timing of the major epidemic between biennia will lead to an average profile that has a lower maximum and a major epidemic of longer duration than any single realization. Also, a single measurement of the error cannot capture all the qualitative features of the model; the sinusoidally forced models have slightly lower errors than the term-time forcing and yet do not reproduce the characteristic abrupt changes that are caused by the beginning and ending of school terms. Thus, while all models should be made to satisfy some best-fit criterion, there is no clear candidate for what this criterion should be.

It should now be clear that if we wish to compare the behaviour of a variety of models, we should first insist that all the models capture the observed dynamics. Here we have fine-tuned our models by fitting the seasonality parameter b_1 . In general, we could fit several parameters by this method, including R_0 and the infectious and incubation periods, although this would be more computationally challenging. By selecting the optimal b_1 , all viable models now possess similar dynamics and hence similar stability properties (all have a stable deterministic biennial cycle); we can therefore compare the effects on persistence of the various model assumptions (using stochastic simulations) without the results being obscured by differing underlying attractors.

3. MEASURES OF PERSISTENCE

In the previous section, for reasons of speed and convenience, we have used deterministic models where population levels are considered to be real numbers and infinitesimal changes occur over infinitesimal time-scales. However, to model extinctions and therefore persistence, we need to move to a stochastic framework (Renshaw 1991), where events occur randomly—but with an underlying rate given by the differential equations—and population levels are always integers. These stochastic models share many of the qualitative features observed in the case-report data for measles, including variation about the attractor (Keeling & Grenfell 1999) and stochastic extinctions. Obviously, due to the random nature of these models, an exact match between reported cases and the model output is virtually impossible. Instead, while checking that the underlying biennial pattern remains, we concentrate on capturing one of the most interesting features of stochastic systems: its persistence.

Two measures of persistence have been used in ecology and epidemiology. One is the number (or total duration) of extinctions in a population with immigration (Bartlett 1957; Grenfell 1992; Keeling 1997), which compares well with localized extinctions in a metapopulation or mainland-island model (Gilpin & Hanski 1991; Hanski & Gilpin 1997). This is the fade-out pattern observed by Bartlett (1957) that leads to the well-known critical community size. However, the actual level of immigration is a very difficult parameter to ascertain and, as shown below, may have a strong impact on the persistence of the disease. The other measure of persistence is defined for an isolated population with no immigration, and is found by calculating the expected time to extinction (often called the first passage time) or by calculating the probability of extinction during a given period (Ludwig 1996; Donalson & Nisbet 1999; Farrington & Grant 1999; Nasell 1999; Saether *et al.* 2000). This measure is a very convenient abstraction as it does not rely on the presence of an unknown external source of imports. However, it does not compare readily with any biological quantity—there are no totally isolated populations—hence we cannot easily compare model results with observations of the real world.

Figure 4a gives the observed pattern of fade-outs from

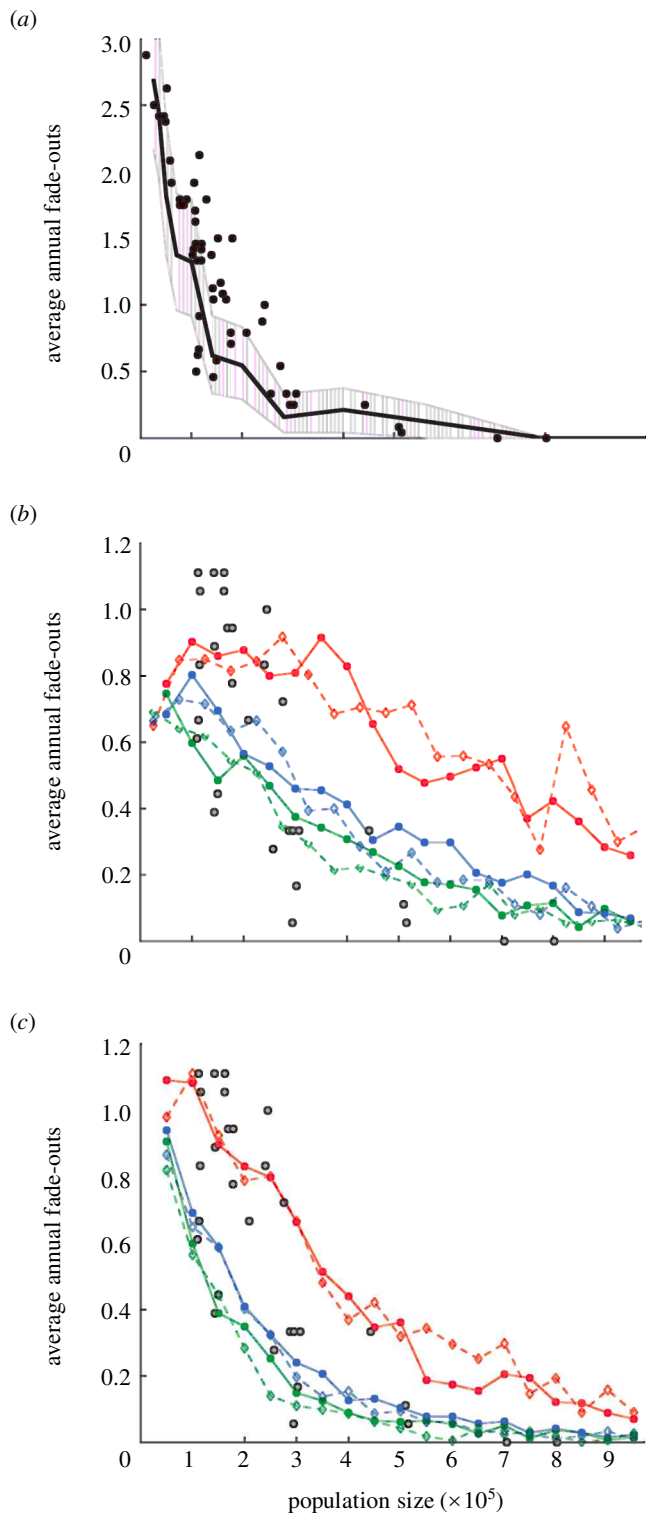


Figure 4. The average number of fade-outs per year against population size. (a) Comparison of the observed results from England and Wales (1944–1968) (dots), against the most accurate mechanistic model to date, the stochastic PRAS model (black line) (Keeling & Grenfell 1997). The grey hashed region is the 95% confidence interval from 200 simulations of a 24 year period (this time-scale was chosen to correspond with the prevaccination era in England and Wales). (b and c) Results from the three different models, exponential SEIR (red lines), gamma SEIR (blue lines) and constant SEIR (green lines). Two types of seasonal forcing were used, term-time forcing (solid line and filled circles) and sinusoidal forcing (dashed line and open diamonds).

England and Wales (1944–1968) together with the results of the pulsed realistic age structured model (PRAS) model (Keeling & Grenfell 1997) that combines age structure and narrow distributions of periods. Figure 4*b,c* shows the fade-out pattern for the six different SEIR models shown in figure 2 (exponential, gamma and constant, all with either sinusoidal or term-time forcing). Following the work of Bartlett (1960), the import rate, Z , of infectious individuals into the population is taken to be:

$$z = k\sqrt{\text{population size.}}$$

In figure 4*a,b*, the proportionality constant, k , is 0.01, whereas in figure 4*c*, the constant is 0.02. Three key observations can be made from these graphs. First, (by comparing figure 4*b,c*) the level of imports is crucial in determining the pattern of fade-outs—obviously as more disease flows into the community the number of fade-outs decreases. Second, comparing figure 4*a* with 4*b*, the extra structural heterogeneity introduced in the age-structured (PRAS) model leads to increased persistence compared with the SEIR models. Finally, from figure 4*b,c* it is clear that the models with narrowly distributed periods (gamma SEIR and constant SEIR) have similar high levels of persistence, whereas the models with exponentially distributed periods exhibit more fade-outs.

For isolated populations with no imports, the probability of extinction during a 30 year period after transients shows different behaviour (figure 5*a*). The distinction between the six models is less clear, although again, the more narrow distributions have slightly higher persistence, as do those with sine wave forcing patterns.

Figure 5*b* shows how difficult it is to compare the results from isolated populations with those populations with imports and to real data. All three lines give the probability of extinction during a 30 year period for the exponential SEIR model—as in figure 5*a*. The black (no imports) and red (with imports) lines are derived from multiple stochastic simulations, starting with the disease present and iterating the model forwards for 30 years. From these two lines, it is clear that imports significantly increase the persistence of measles in any community. By contrast, the blue line is taken from a single long simulation and shows the probability that, upon reintroduction, measles persists for 30 years. The lower level of persistence for this model formulation is a strong indication that extinctions are temporally correlated; after a local extinction, any subsequent import is most likely to give rise to a short-duration epidemic. Thus, the theoretically appealing probability of extinction (calculated from multiple simulations) cannot even be used to inform us about the duration of persistence in real populations (that represent a single long simulation), and hence, cannot be compared with the observed case reports.

The grey circles are the number of fade-outs from the England and Wales data before vaccination. (a and b) average $0.01\sqrt{\text{pop.size imports per year}}$, whereas (c) averages $0.02\sqrt{\text{pop.size}}$. The results are the average of 10 simulations of 100 years after a 20 year transient period. We note that exponential SIR and gamma SIR have persistence levels comparable with their SEIR counterpart.

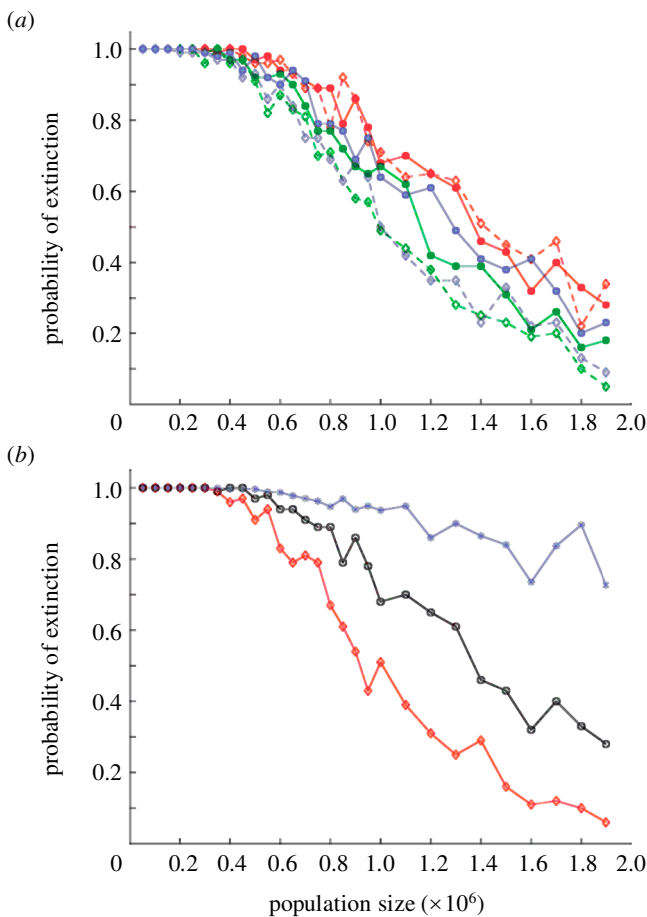


Figure 5. Probability of extinction during a 30 year realization for the exponential SEIR model. We note that although the same qualitative features hold, the differences shown here are far less dramatic for models with more constant infectious periods. (a) Results are for 100 simulations of 30 years with no imports, after a transient period of 10 years with imports (labelled as in figure 4). (b) Comparison between exponential SEIR models, with (black) and without (red) imports. The blue line shows the probability that an epidemic/endemic period lasts for more than 30 years, results are from 10 simulations of 300 years each.

4. CONCLUSIONS

If we wish to evaluate the performance of a model, then all aspects of its behaviour should be compared with observations. To assess the persistence of various disease models we must always return to the case reports. For measles, we must insist that the (deterministic) model is a good description of the disease, matching the observed biennial pattern of cases; only then can the persistence of the (stochastic) model be judged. Ideally, one should seek a stochastic model that matches the observed behaviour at a range of population sizes, birth rates and vaccination levels. For diseases such as whooping cough, where stochasticity is fundamental to the observed dynamics (Keeling *et al.* 2001; Rohani *et al.* 2001), such a comprehensive search may be vital, although computationally intensive.

By fitting the seasonality, b_1 , so as to minimize the error between the deterministic pattern and the observed bien-

nial cycles, three main features are revealed. First, the SIR model cannot readily capture the dynamics when the more realistic constant infectious period is used, although interestingly a discrete time SIR-type model that implicitly assumes constant infectious periods provides one of the most accurate models of measles (Finkenstädt & Grenfell 2000). Hence subtle differences between model choices can have a dramatic effect on the accuracy of results. Second, in agreement with the theoretical predictions of Grossman (1980) and the simulations of Lloyd (2001), the models with less variable infectious periods (the constant and gamma distributions) are less stable and therefore require far lower levels of seasonality to force the resonance of biennial cycles. Finally, the models with sinusoidal forcing provide a slightly better fit to the data, despite the fact that they fail to reproduce the dramatic changes driven by the greater mixing during school terms. This can be explained by our over-simplistic form for the term-time forcing; the presence of age-structure and non-random mixing means that the changes in contact rate due to the opening and closing of schools become smeared out (Finkenstädt & Grenfell 2000). We note that an age-structured model with term-time forcing and constant infectious periods (the PRAS model, Keeling & Grenfell (1997)) has the lowest error of all. We therefore believe that the more mechanistic term-time forcing is the more appropriate form of seasonality.

To examine questions of disease persistence we need to move to a stochastic (event-driven) model where the individual nature of the population becomes important. Two main measures of persistence were compared, the probability of extinction and the number of fade-outs. Although considering the probability of extinction (or time to extinction) of an isolated population is more intuitively appealing and mathematically tractable (Nasell 1999; Andersson & Britton 2000), there are no observational data to compare with model results. We are therefore forced to look at the fade-out pattern for populations with a realistic level of infectious immigration. This comparison with data is vital if we want to obtain the most accurate model of measles and not just a model that persists well. The results of many stochastic simulations support the earlier work of Keeling & Grenfell (1997), showing that the measles models with narrow distributions (constant and gamma) possess far greater levels of persistence. It is interesting to note that for diseases without seasonality the situation would be reversed; the greater stability of the exponential period would lead to greater persistence.

In conclusion, the ideology of this paper should hold when comparing various mathematical models for any biological system. There is often very little choice in parameter values if our models are to mimic the observed behaviour; it is the observables rather than parameters that should be fixed to allow fair comparisons of different models.

This research was supported by The Royal Society (M.J.K.) and the Wellcome Trust (B.T.G.).

APPENDIX A

Throughout the models we set the birth and death rates to be equal ($B = d = 5 \times 10^{-5} \text{ days}^{-1}$), so that the popu-

lation size remains constant. We also modified the value of b_0 , such that the average R_0 is always 17 irrespective of the value of b_1 .

(i) *Standard (exponential) SEIR*

$$\frac{dS}{dt} = B - \beta(t)SI - dS,$$

$$\frac{dE}{dt} = \beta(t)SI - aE - dE,$$

$$\frac{dI}{dt} = aE - gI - dI,$$

$$\frac{dR}{dt} = gI - dR.$$

(ii) *Gamma SEIR*

$$\frac{dS}{dt} = B - \beta(t)S \sum_{n=1}^N I_n - dS,$$

$$\frac{dE_1}{dt} = \beta(t)S \sum_{n=1}^N I_n - aME_1 - dE_1,$$

$$\frac{dE_n}{dt} = aME_{n-1} - aME_n - dE_n \quad \forall 2 \leq n \leq M,$$

$$\frac{dI_1}{dt} = aME_M - gNI_1 - dI_1,$$

$$\frac{dI_n}{dt} = gNI_{n-1} - gNI_n - dI_n \quad \forall 2 \leq n \leq N,$$

$$\frac{dR}{dt} = dNI_N - dR.$$

This has subdivided the exposed and infectious class into M and N distinct subclasses, respectively. Throughout we have used $M = 8$ and $N = 5$ such that individuals spend on average one day in each class.

(iii) *Constant SEIR*

$$\frac{dS}{dt} = B - \beta(t)S \int_{T_0}^{T_1} I(t,\tau) d\tau - dS,$$

$$I(t,0) = \beta(t)S \int_{T_0}^{T_1} I(t,\tau) d\tau,$$

$$\frac{\partial I}{\partial t} = -dI(t,\tau) - \frac{\partial I}{\partial \tau},$$

$$\frac{dR}{dt} = I(t,T_1) - dR,$$

where T_0 is the exposed period and $T_1 - T_0$ is the infectious period. This constant period model is equivalent to the gamma model when M and N tend to infinity. Instead of writing the model as a partial differential equation, it can also be written as a time delay.

$$\frac{dS}{dt} = B - \beta(t)SI - dS,$$

$$\frac{dI}{dt} = \beta(t - T_0)S(t - T_0)I(t - T_0)e^{-dT_0}$$

$$- \beta(t - T_1)S(t - T_1)I(t - T_1)e^{-dT_1} - dI,$$

$$\frac{dR}{dt} = \beta(t - T_1)S(t - T_1)I(t - T_1)e^{-dT_1} - dR.$$

REFERENCES

Anderson, D. & Watson, R. 1980 On the spread of a disease with gamma distributed latent and infectious periods. *Biometrika* **67**, 191–198.

Anderson, R. M. & May, R. M. 1979 Population biology of infectious diseases part I. *Nature* **280**, 361–366.

Anderson, R. M. & May, R. M. 1992 *Infectious diseases of humans*. Oxford University Press.

Andersson, H. & Britton, T. 2000 Stochastic epidemics in dynamic populations: quasi-stationarity and extinction. *J. Math. Biol.* **41**, 559–580.

Andersson, H. & Djehiche, B. 1998 A threshold limit theorem for the stochastic logistic epidemic. *J. Appl. Prob.* **35**, 662–670.

Aron, J. L. & Schwartz, I. B. 1984 Seasonality and period-doubling bifurcations in an epidemic model. *J. Theor. Biol.* **110**, 665–679.

Bailey, N. J. T. 1956 On estimating the latent and infectious periods of measles, 1. Families with two susceptibles only. *Biometrika* **43**, 15–22.

Bartlett, M. S. 1956 Deterministic and stochastic models for recurrent epidemics. *Proc. 3rd Berkeley Symp. Math. Stats. Prob.* **4**, 81–108.

Bartlett, M. S. 1957 Measles periodicity and community size. *J. R. Stat. Soc. A* **120**, 48–70.

Bartlett, M. S. 1960 The critical community size for measles in the U.S. *J. R. Stat. Soc. A* **123**, 37–44.

Bascompte, J. & Rodriguez-Trelles, F. 1998 Eradication thresholds in epidemiology, conservation biology and genetics. *J. Theor. Biol.* **192**, 415–418.

Black, F. L. 1966 Measles endemicity in insular populations: critical community size and its evolutionary implications. *J. Theor. Biol.* **11**, 207–211.

Bolker, B. M. 1993 Chaos and complexity in measles models: a comparative numerical study. *Inst. Math. Appl. J. Math. Appl. Med. Biol.* **10**, 83–95.

Bolker, B. M. & Grenfell, B. T. 1995 Space, persistence and dynamics of measles epidemics. *Phil. Trans. R. Soc. Lond. B* **348**, 309–320.

Bolker, B. M. & Grenfell, B. T. 1996 Impact of vaccination on the spatial correlation and persistence of measles dynamics. *Proc. Natl Acad. Sci. USA* **93**, 12 648–12 653.

Caraco, T., Duryea, M., Gardner, G., Maniatty, W. & Szymanski, B. K. 1998 Host spatial heterogeneity and extinction of an SIS epidemic. *J. Theor. Biol.* **192**, 351–361.

Donalson, D. D. & Nisbet, R. M. 1999 Population dynamics and spatial scale: effects of system size on population persistence. *Ecology* **80**, 2492–2507.

Earn, D. J. D., Rohani, P. & Grenfell, B. T. 1998 Persistence, chaos and synchrony in ecology and epidemiology. *Proc. R. Soc. Lond. B* **265**, 7–10.

Earn, D. J. D., Rohani, P., Bolker, B. M. & Grenfell, B. T. 2000 A simple model for complex dynamical transitions in epidemics. *Science* **287**, 667–670.

Farrington, C. P. & Grant, A. D. 1999 The distribution of time to extinction in subcritical branching processes: applications to outbreaks of infectious disease. *J. Appl. Prob.* **36**, 771–779.

Ferguson, N. M., Anderson, R. M. & May, R. M. 1997 Scale, persistence and synchronicity: measles as a paradigm of a

- spatially-structured ecosystem. In *Spatial ecology: the role of space in population dynamics and interspecific interactions* (ed. D. Tilman & P. Kareiva). Princeton University Press.
- Finkenstädt, B. & Grenfell, B. 2000 Time series modelling of childhood diseases: a dynamical systems approach. *J. R. Stat. Soc. C* **49**, 187–205.
- Gilpin, M. E. & Hanski, I. A. 1991 *Metapopulation dynamics: empirical and theoretical investigations*. San Diego: Academic Press.
- Grenfell, B. T. 1992 Chance and chaos in measles dynamics. *J. R. Stat. Soc. B* **54**, 383–398.
- Grenfell, B. T., Bolker, B. M. & Kleczkowski, A. 1995 Seasonality and extinction in chaotic metapopulations. *Proc. R. Soc. Lond. B* **259**, 97–103.
- Grossman, Z. 1980 Oscillatory phenomenon in a model of infectious diseases. *Theor. Pop. Biol.* **18**, 204–243.
- Hanski, I. A. & Gilpin, M. E. (eds) 1997 *Metapopulation biology, ecology, genetics and evolution*. San Diego: Academic Press.
- Hanski, I., Pakkala, T., Kuussaari, M. & Lei, G. C. 1995 Metapopulation persistence of an endangered butterfly in a fragmented landscape. *Oikos* **72**, 21–28.
- Holyoak, M. & Lawler, S. P. 1996 Persistence of an extinction-prone predator–prey interaction through metapopulation dynamics. *Ecology* **77**, 1867–1879.
- Hope-Simpson, R. E. 1952 Infectiousness of communicable diseases in the household. *Lancet* **2**, 549–554.
- Keeling, M. J. 1997 Modelling the persistence of measles. *Trends Microbiol.* **5**, 513–518.
- Keeling, M. J. 2000 Metapopulation moments: coupling, stochasticity and persistence. *J. An. Ecol.* **69**, 725–736.
- Keeling, M. J. & Grenfell, B. T. 1997 Disease extinction and community size: modeling the persistence of measles. *Science* **275**, 65–67.
- Keeling, M. J. & Grenfell, B. T. 1999 Stochastic dynamics and a power law for measles variability. *Phil. Trans. R. Soc. Lond. B* **354**, 769–776.
- Keeling, M. J., Rohani, P. & Grenfell, B. T. 2001 Seasonally-forced disease dynamics explored as switching between attractors. *Physica D* **148**, 317–335.
- Kermack, W. O. & McKendrick, A. G. 1927 A contribution to the mathematical theory of epidemics. *Proc. R. Soc. Lond. A* **115**, 700–721.
- Lande, R. 1993 Risks of population extinction from demographic and environmental stochasticity and random catastrophes. *Am. Nat.* **142**, 911–927.
- Lloyd, A. L. 2001 Destabilization of epidemic models with the inclusion of realistic distributions of infectious periods. *Proc. R. Soc. Lond. B* **268**, 985–993.
- Ludwig, D. 1996 The distribution of population survival times. *Am. Nat.* **147**, 506–526.
- Marion, G., Renshaw, E. & Gibson, G. 2000 Stochastic modelling of environmental variation for biological populations. *Theor. Pop. Biol.* **57**, 197–217.
- May, R. M. & Anderson, R. M. 1979 Population biology of infectious diseases part II. *Nature* **280**, 455–461.
- Nasell, I. 1999 On the time to extinction in recurrent epidemics. *J. R. Stat. Soc. B* **61**, 309–330.
- Olsen, L. F. & Schaffer, W. M. 1990 Chaos versus noisy periodicity: alternative hypotheses for childhood epidemics. *Science* **249**, 499–504.
- Ouborg, N. J. 1993 Isolation, population-size and extinction—the classical and metapopulation approaches applied to vascular plants along the Dutch Rhine-system. *Oikos* **66**, 298–308.
- Rand, D. A. & Wilson, H. B. 1991 Chaotic stochasticity—a ubiquitous source of unpredictability in epidemics. *Proc. R. Soc. Lond. B* **246**, 179–184.
- Renshaw, E. 1991 *Modelling biological populations in space and time*. Cambridge University Press.
- Rohani, P., Keeling, M. J. & Grenfell, B. T. 2001 The Interplay between determinism and stochasticity in childhood diseases. *Am. Nat.* (In the press.)
- Saether, B. E., Engen, S., Lande, R., Arcese, P. & Smith, J. N. M. 2000 Estimating the time to extinction in an island population of song sparrows. *Proc. R. Soc. Lond. B* **267**, 621–626.
- Schenzle, D. 1984 An age-structured model of pre- and post-vaccination measles transmission. *Inst. Math. Appl. J. Math. Appl. Med. Biol.* **1**, 169–191.
- Stacey, P. B. & Taper, M. 1992 Environmental variation and the persistence of small populations. *Ecol. Applications* **2**, 18–29.
- Sutcliffe, O. L., Thomas, C. D., Yates, T. J. & Greatorex-davies, J. N. 1997 Correlated extinctions, colonizations and population fluctuations in a highly connected ringlet butterfly metapopulation. *Oecologia* **109**, 235–241.
- Swinton, J. 1998 Extinction times and phase transitions for spatially structured closed epidemics. *Bull. Math. Biol.* **60**, 215–230.
- Swinton, J. & Gilligan, C. A. 1996 Dutch elm disease and the future of the elm in the UK: a quantitative analysis. *Proc. R. Soc. Lond. B* **351**, 605–615.
- Tilman, D. 1994 Competition and biodiversity in spatially structured habitats. *Ecology* **75**, 2–16.
- van Herwaarden, O. A. 1997 Stochastic epidemics: the probability of extinction of an infectious disease at the end of a major outbreak. *J. Math. Biol.* **35**, 793–813.

As this paper exceeds the maximum length normally permitted, the authors have agreed to contribute to production costs.